Engineered Science
DOI: https://dx.doi.org/10.30919/es1667

Optical Diagnosis of Liver Cirrhosis and Hepatocellular Carcinoma using Machine Learning-Assisted Serum Raman Spectroscopy

Sasikan Borwornmote,[1] Peeraya Suksuratin,[1] Rutchanee Rodpai,[2,3] Wattana Sukeepaisarnjaroen,[4] Pewpan M. Intapan,[2,3] Wanchai Maleewong[2,3] and Oranat Chuchuen[1,3,5,*]

Abstract

This study introduces a simple yet effective method that integrates Raman spectroscopy (RS) with support vector machines (SVM) for the detection and differentiation of hepatocellular carcinoma (HCC), cirrhosis, and healthy individuals via serum analysis. RS revealed a prominent collagen marker band at approximately 1246 cm^{-1}, showing significant elevation in HCC and cirrhotic patients compared to healthy controls. Furthermore, serum levels of aromatic amino acids—including tryptophan (757, 878 cm^{-1}), tyrosine (831, 853 cm^{-1}), and phenylalanine (1004 cm^{-1})—and cholesterol (548, 699 cm^{-1}) were significantly elevated in patients with cirrhosis and HCC compared to the healthy group. In contrast, β-carotene levels (1157, 1527 cm^{-1}) were significantly reduced in both cirrhotic and HCC patients. Binary machine learning classifications (cirrhosis vs. healthy, HCC vs. healthy, and cirrhosis vs. HCC) achieved 83.3–92.0% sensitivity, 89.3–95.3% specificity, and AUC values of 0.929–0.980, validated using 5-fold subject-wise and leave-one-subject-out (LOSO) cross-validations. Moreover, multiclass classification of the three groups correctly assigned individual subjects to their respective categories, achieving accuracies of 80.0–89.3% for healthy, 81.3–84.4% for cirrhosis, and 85.3–93.3% for HCC. The integration of RS and machine learning offers a simple, rapid, and cost-effective diagnostic method for the serum-based differentiation and screening of cirrhosis and HCC.

Keywords: Hepatocellular carcinoma (HCC); Liver cancer; Liver cirrhosis; Raman spectroscopy; Machine learning.
Received: 28 February 2025; Revised: 24 July 2025; Accepted: 02 August 2025
Article type: Research article.

1. Introduction

Liver cirrhosis is one of the most advanced forms of liver disease, characterized by persistent and progressive scarring (fibrosis) of liver tissue, often due to chronic inflammation. This scarring can lead to changes in hepatocytes, increasing the risk of genetic alterations that may eventually result in hepatocellular carcinoma (HCC).[1] The global burden of cirrhosis has been increasing, with the number of deaths rising from approximately 1 million in 1990 to 1.5 million in 2019, with an estimated 1.43 million deaths reported in 2021, highlighting the persistent and substantial mortality burden.[2,3] Furthermore, it is estimated that over one hundred million people live with compensated cirrhosis, the majority of whom are asymptomatic, leaving them at risk of silent progression to decompensation or HCC.[4] HCC is the most common form of primary liver cancer, accounting for approximately 830,000 deaths globally in 2020, making it the fourth leading cause of cancer-related mortality worldwide.[5] HCC demonstrates significant regional and demographic variability in both incidence and mortality, with particularly pronounced increases observed in developing nations.[4,6] It is widely recognized that 80%-90% of HCC cases occur in individuals with underlying liver cirrhosis.[7] In certain instances, cirrhosis and HCC can manifest with remarkably similar hepatocyte morphology, presenting a significant diagnostic challenge, especially in distinguishing between end-stage cirrhosis and HCC.[8] These diagnostic difficulties complicate treatment decisions and adversely impact prognostic outcomes, necessitating the use of comprehensive clinical evaluation, advanced imaging techniques, serum biomarkers and sometimes sophisticated histopathological methods to accurately distinguish between the two conditions. Consequently, there is a critical need for the development of a rapid and straightforward screening technique capable of distinguishing between these two types of liver disease and differentiating them from healthy individuals. This could improve early diagnosis and treatment and potentially reduce

[1]*Biomedical Engineering Program, Faculty of Engineering, Khon Kaen University, Khon Kaen, 40002, Thailand*
[2]*Department of Parasitology, Faculty of Medicine, Khon Kaen University, Khon Kaen, 40002, Thailand*
[3]*Mekong Health Science Research Institute, Khon Kaen University, Khon Kaen, 40002, Thailand*

mortality rates associated with liver cirrhosis and HCC.

Although alpha-fetoprotein (AFP) is widely used as a biomarker for the detection of HCC and the monitoring of liver disease, its application is limited by several factors. These include low sensitivity and specificity, variability in measurement methods, and the influence of patient characteristics and AFP cut-off values.[9] Recently, prothrombin induced by vitamin K absence or antagonist-II (PIVKA-II) has been investigated as a blood biomarker for HCC screening, especially in cases where AFP is negative, providing a more accurate diagnosis than AFP alone. However, elevated serum levels of PIVKA-II are not exclusive to HCC and can also be observed in other conditions, such as gastric cancer, renal failure, and inflammatory bowel disease, which complicates its use as a sole prognostic tool.[10] Moreover, the cost-effectiveness of using PIVKA-II in routine screening is still under debate and remains a challenge,[11] necessitating further research to enhance its clinical utility.

Imaging techniques are widely used for diagnosing liver diseases, but they face limitations that affect diagnostic accuracy and reliability, especially in resource-limited settings. The high cost of advanced imaging modalities like MRI and CT scans restricts their availability in developing countries, where access to advanced medical facilities is often limited.[12] Furthermore, the effective use of these techniques requires skilled radiologists and technicians, who are frequently in short supply in these regions, leading to misinterpretation of imaging results and delayed diagnoses.[13] Although ultrasonography is more cost-effective compared to MRI and CT scans, it is generally less effective, particularly in obese patients.[14] Additionally, the quality and accuracy of ultrasound results heavily depend on the operator's skill and experience, resulting in potential variability.[14] Given these challenges, especially in resource-constrained areas, there has been a growing focus on developing non-complex and affordable methods for screening cirrhosis and HCC.

Raman spectroscopy (RS) and its advanced variants, such as Surface-Enhanced Raman Spectroscopy (SERS), have emerged as promising tools for disease diagnostics. RS operates on the principle of inelastic scattering of photons when they interact with molecules. The energy of these Raman-scattered photons shifts from that of the incident light, producing spectra that serve as unique fingerprints for identifying different molecular structures. RS offers marker-free, instantaneous, and non-destructive detection of molecules. It has been extensively applied in biomedical research and medicine, including studies on pharmaceutical agents,[15-17] cannabinoids,[18] parasitology,[19] nanoparticle-bacteria interactions,[20] regenerative medicine,[21] and the detection of cancers, such as breast cancer,[22] oral cancer,[23] and cholangiocarcinoma.[24]

In the context of liver diseases, RS and SERS have been explored for the detection of fatty liver disease,[25] cirrhosis,[26] and liver cancer[27,28] through serum and plasma analysis and tissue imaging.[29] A study has employed the SERS technique to differentiate between patients with cirrhosis and those with HCC using serum samples.[30] However, compared to conventional RS, SERS faces challenges in terms of repeatability, reproducibility, and the complexity of preparing metallic nanostructure substrates, which are often costly and require sophisticated equipment.[31] The interactions between metallic SERS substrates and molecules in biofluids also raise concerns about the reliability of information obtained from SERS for therapeutic or diagnostic use.[32] To our knowledge, no studies have yet employed conventional RS combined with machine learning classification to simultaneously differentiate among three groups—HCC patients, individuals with cirrhosis, and healthy individuals—alongside biomolecular analysis of their serum Raman spectra.

Despite its potential, conventional Raman spectroscopy alone may face challenges when applied to complex biological systems due to overlapping spectral features and subtle biomolecular variations across disease stages. To address these challenges and extract diagnostically relevant patterns from high-dimensional spectral data, machine learning (ML) a subdomain of artificial intelligence, techniques have been increasingly integrated with spectroscopic analysis.[33] ML facilitates learning from data to make predictions or decisions without explicit programming. It has been widely adopted across various domains, including finance, manufacturing, agriculture, and most notably, healthcare. Recent studies have leveraged ML for human activity classification,[34] which can support personalized health monitoring, as well as for predicting pandemic-related fatality rates,[35] highlighting the growing impact of data-driven models in health-related applications. In the biomedical field, ML has proven valuable in disease diagnosis, patient stratification, drug discovery, and medical imaging, largely due to its capacity to analyze complex, high-dimensional data.[36] One of its emerging applications is in spectral discrimination, where ML enhances sensitivity, specificity, and automation while supporting rapid and cost-effective analysis. It remains highly effective even with small datasets, making it ideal for health-related investigations where sample sizes are limited.[37] Moreover, integrating ML with portable, cloud-connected near-infrared spectroscopy has demonstrated high classification accuracy and reliable quantitative predictions in complex biological mixtures.[38] This underscores its potential for fast and non-destructive diagnostics in real-world scenarios. Collectively, these advantages highlight the practical value of ML-based spectral analysis in healthcare and point-of-care diagnostics.

Building on these strengths, this study applied a label-free conventional Raman spectroscopy (RS) technique to assess biomolecular differences in serum among patients with HCC,

[4]*Department of Medicine, Faculty of Medicine, Khon Kaen University, Khon Kaen, 40002, Thailand*

[5]*Department of Chemical Engineering, Faculty of Engineering, Khon Kaen University, Khon Kaen, 40002, Thailand*

**Email:* oranat@kku.ac.th (Chuchuen. O)

Table 1: Demographic and Clinical Characteristics of Cirrhosis and HCC Patients.

Demographic	Age (years)	Gender		Child-Pugh			Barcelona Clinic Liver Cancer (BCLC) staging system			
		Male	Female	A	B	C	A	B	C	D
Cirrhosis (n = 30)	60.13 ± 9.28	20 (66.7%)	10 (33.3%)	27 (90.0%)	2 (6.7%)	1 (3.3%)				
HCC (n = 30)	60.77 ± 9.61	24 (80.0%)	6 (20.0%)				6 (20.0%)	14 (46.7%)	7 (23.3%)	3 (10.0%)

individuals with cirrhosis, and healthy controls. The RS method identified distinct biomolecular variations in serum across the three groups, revealing specific spectral fingerprints and marker bands that facilitate disease differentiation. To enhance the diagnostic classification, the spectral analysis incorporated a machine learning technique, combining principal component analysis (PCA) with support vector machines (SVM). This PCA-SVM approach was employed for both two-group and simultaneous three-group classifications. The diagnostic performance of the model was assessed using various metrics, including sensitivity, specificity, accuracy, and the area under the receiver operating characteristic (ROC) curves. This machine learning-enhanced optical method offers a simple, rapid, and cost-effective means of screening and diagnosing cirrhosis and HCC, demonstrating potential for improving clinical diagnosis of these liver diseases.

2. Materials and methods

2.1 Sample size calculation

The sample size was estimated using Cochran's sample size formula to ensure adequate statistical power and precision:

$$n_0 = \frac{Z^2 p(1-p)}{e^2}$$ [39]

where:

n_0 is the minimum required sample size.

Z is the Z-score corresponding to the desired confidence level.

p is the prevalence of the condition of interest in the population.

e is the acceptable margin of error.

A 95% confidence level (Z = 1.96) and 1% margin of error (e = 0.01) were applied. Prevalence estimates were based on recent population-level data from Thailand to ensure contextual relevance. For cirrhosis, a nationwide registry study reported an age-standardized prevalence of 75.3 per 100,000 population, corresponding to p = 0.00075.[40] For HCC, an age-standardized incidence rate of 22.3 per 100,000 per year, yielded an estimated prevalence of 0.05% (p = 0.0005).[41] Based on Cochran's formula, the minimum required sample sizes were approximately 29 for cirrhosis and 20 for HCC. To standardize group sizes and exceed the minimum requirements, 30 participants were selected for each group. While resource constraints were considered, this sample allocation supports robust model training, fair group comparisons, and reliable evaluation of the classification model's performance.

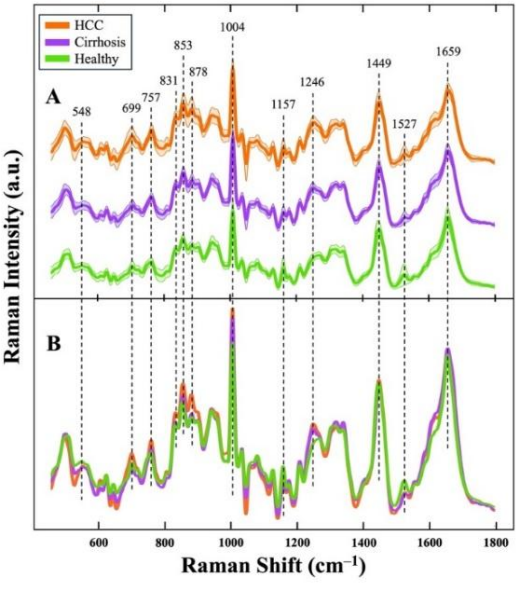

Fig. 1: Comparison of mean Raman spectra among hepatocellular carcinoma (HCC), cirrhosis, and healthy groups (n = 30, each group). A. The Raman spectra for each group were averaged and offset for clear visualization. Solid lines represent the mean intensities, while shaded areas indicate the standard deviations. B. The average serum Raman spectra for all groups are superimposed. Dashed lines denote the positions of the major peaks observed in the serum Raman spectra across the three groups.

2.2 Collection and preparation of serum specimens

This study utilized leftover serum specimens from cirrhosis patients (n = 30) and HCC patients (n = 30) who visited Srinagarind Hospital, Faculty of Medicine, Khon Kaen University, Khon Kaen, Thailand, for routine investigations before surgery. Serum samples from the healthy group (n = 30) were randomly selected from a frozen biobank at the Department of Parasitology, Faculty of Medicine, Khon Kaen University. A summary of the demographic and clinical data of cirrhosis and HCC is presented in Table 1. All data were completely anonymized. The collection and measurement of the serum samples used in this study were approved by the Khon Kaen University Ethics Committee for Human Research (HE641114), in compliance with the Declaration of Helsinki.

Table 1 summarizes the demographic and clinical characteristics of the cirrhosis and HCC cohorts enrolled in this study. The average age of the healthy group, cirrhosis patients, and HCC patients was 64 ± 7.25, 60.13 ± 9.28, and 60.77 ± 9.61 years, respectively. Given this distribution, the age range selected for this study primarily aligns well with the reported peak incidence of liver cirrhosis (50–69 years)[42] and HCC (65-68 years)[43] across mixed etiologies. This study also included both male and female participants, which enhances the comprehensiveness of the analysis and helps minimize gender-related bias, thereby improving the general applicability of the findings. A higher proportion of male patients was observed in both groups, reflecting known epidemiological trends in liver diseases. This gender distribution is consistent with previous reports demonstrating male predominance in both cirrhosis and HCC due to hormonal and lifestyle-related risk factors.[44,45] Clinically, 90% of cirrhosis patients were classified as Child–Pugh A, reflecting well-compensated liver function. The HCC group was stratified by the Barcelona Clinic Liver Cancer (BCLC) staging system, with most patients in stage B (46.7%), followed by C (23.3%), A (20.0%), and D (10.0%). Critically, the cohort spanned all stages of disease progression, with a predominance of early-stage cirrhosis and early to intermediate HCC. This broad representation enables a robust evaluation of the model's diagnostic performance in clinically relevant scenarios, particularly for initial-stage detection. Such a representative sample distribution supports the development of generalizable machine learning models for liver disease diagnosis across varying disease stages.

2.3 Acquisition of Raman spectral data

The tube containing frozen serum was thawed at 4 °C before undergoing Raman measurement. A serum volume of 2.3 µl was deposited into the well of a flat washer, which was mounted on a mirror-grade stainless steel plate. It was then covered with a quartz coverslip (R52500, Esco Optics, Oak Ridge, NJ) and placed on the stage of a Horiba XploRA PLUS confocal Raman microscope (Horiba Jobin Yvon, Northampton, UK) to obtain the Raman spectra of the sample. The experiment utilized a grating of 1,200 gr/mm, a slit width of 200 µm, and a hole diameter of 500 µm. A 785-nm near-infrared (NIR) excitation laser was used to prevent sample burning and minimize fluorescence from organic compounds. The laser light was focused onto the sample surface using a 50x objective lens (LMPLFL50X, Olympus, St. Joseph, MI). The stainless-steel plate and quartz coverslip were cleansed with Virkon solution before each measurement for disinfection. Raman spectra were acquired independently five times for each sample, covering the spectral range of 0 to 2,000 cm^{-1}, with a 60-second acquisition period for each measurement.

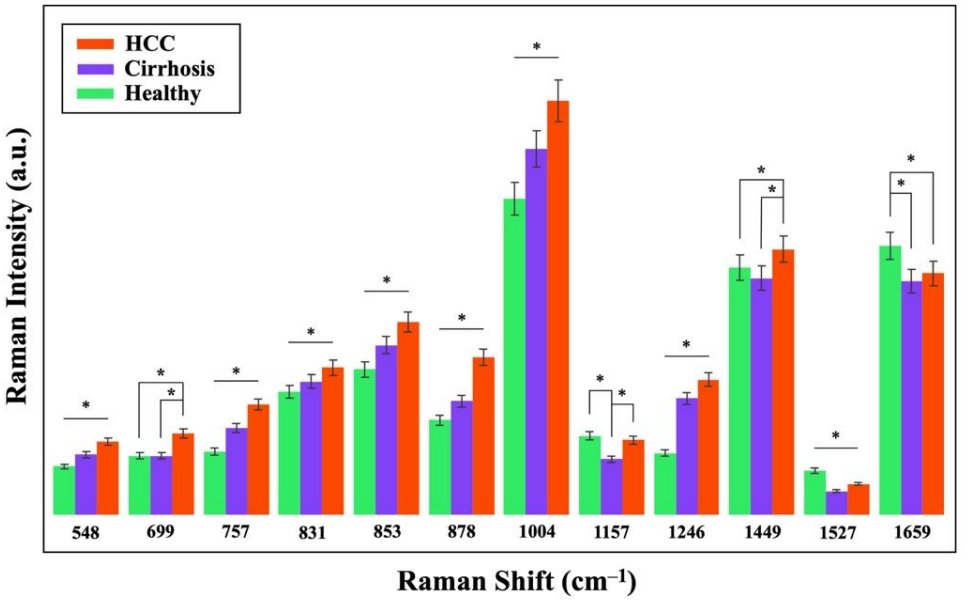

Fig. 2: Comparison of Raman peak heights of major Raman bands in serum specimens from hepatocellular carcinoma (HCC) patients, cirrhosis patients, and healthy subjects. The symbol (*) indicates statistically significant differences between groups ($p < 0.05$).

Table 2: Tentative assignments of major peaks found in Raman spectra of HCC, cirrhosis (LC) and healthy (H) sera, based on the literature.[24,46-52]

Raman shift (cm^{-1})	Assigned vibrational mode	Assigned biomolecule	Significant differences between groups		
			HCC-LC	HCC-H	LC-H
548	Ring CH_2 bending	Cholesterol	✓	✓	✓
699	Steroid ring stretching	Cholesterol	✓	✓	-
757	Symmetric ring breathing	Tryptophan	✓	✓	✓
831	O-P-O stretching	Tyrosine	✓	✓	✓
853	Ring breathing, C−C stretching	Tyrosine, proline	✓	✓	✓
878	C–C stretching	Tryptophan	✓	✓	✓
1004	C–C symmetric ring breathing	Phenylalanine	✓	✓	✓
1157	C–C stretching	β-carotene	✓	-	✓
1246	C-N stretching	Amide III of collagen (proline-rich)	✓	✓	✓
1449	CH_3CH_2 deformation, C–H vibration	Proteins, lipids	✓	✓	-
1527	C=C stretching	β-carotene	✓	✓	✓
1659	C=O stretching	Amide I of protein	-	✓	✓

2.4 Raman spectral data processing

Raw Raman spectra were exported to MATLAB software (MathWorks, Natick, MA) for spectral analysis. Each spectrum was processed by subtracting a fourth-degree polynomial fit to reduce noise and eliminate the fluorescence background. The spectra were then normalized based on the average intensity across all wavenumbers and smoothed using a Savitzky-Golay filter. The peak heights were analyzed using the Peak Analyzer tool in OriginLab software (OriginLab Corporation, Northampton, MA, USA) by fitting each spectrum with a Gaussian function.

2.5 Data analysis by machine learning

The classification method involved dimensionality reduction via principal component analysis (PCA), followed by supervised classification using support vector machines (SVM). Initially, the processed Raman spectra were analyzed using PCA, which reduced dimensionality by identifying the principal axes of variance in a dataset. This technique summarizes high-dimensional data by generating principal components (PCs) that capture most of the variability. These transformed spectral data, represented as PCs, were then used for machine learning analysis. SVM with a radial basis function (RBF) kernel was implemented in Python (Jupyter Notebook 6.1.4, Anaconda Navigator). For visualization purposes, a 70/30 subject-wise train–test split was used. PCA was fitted using the training data, and test data were subsequently projected onto the same PC space for visualization. To avoid overfitting and ensure fair evaluation, two subject-level cross-validation strategies were applied. First, 5-fold subject-wise cross-validation was conducted to assess model reproducibility and performance consistency, ensuring exclusive subject-level separation between training and test sets. Additionally, leave-one-subject-out (LOSO) cross-validation was employed to rigorously evaluate generalizability to unseen individuals. In this approach, all samples from a single subject were held out as the test set in each fold. Model performance was evaluated using accuracy, sensitivity, specificity, and the area under the receiver operating characteristic curve (AUC). ROC curves and corresponding metrics were computed from cross-validated predictions.

3. Results and discussion

Raman spectroscopy has identified several distinctive serum peaks associated with hepatocellular carcinoma (HCC) and cirrhosis that were distinguishable from those seen in health individuals. This differentiation was evident from comparing the mean serum Raman spectra and peak intensities among HCC patients, cirrhosis patients, and healthy individuals, as shown in Fig. 1 and Fig. 2. Moreover, Table 2 provides tentative assignments of vibrational modes and corresponding biomolecules for the major Raman peaks identified. Since the human liver is responsible for protein synthesis, the manufacture of vital substances, and the production of essential biomolecules, changes in the biomolecular composition due to abnormal liver function could be observed in the characteristic Raman bands. Specifically, Raman spectral analysis revealed that serum levels of collagen (1246 cm^{-1}) and aromatic amino acids—namely, tryptophan (757 and 878 cm^{-1}), tyrosine (831 and 853 cm^{-1}), and phenylalanine (1004 cm^{-1})—along with cholesterol (548 and 699 cm^{-1}) were significantly elevated in patients with cirrhosis and HCC compared to healthy controls. Conversely, the β-carotene level (1157 and 1527 cm^{-1}) was significantly lower in the cirrhosis group compared to the healthy group.

The most notable Raman spectral difference among HCC, cirrhosis, and healthy sera appeared around 1246 cm^{-1}, within the amide III band of collagen, which represents a proline-rich region.[47,53] The 1246 cm^{-1} peak was present in both cirrhosis and HCC sera with significantly higher intensity than in the healthy group, in which the peak was absent. This finding

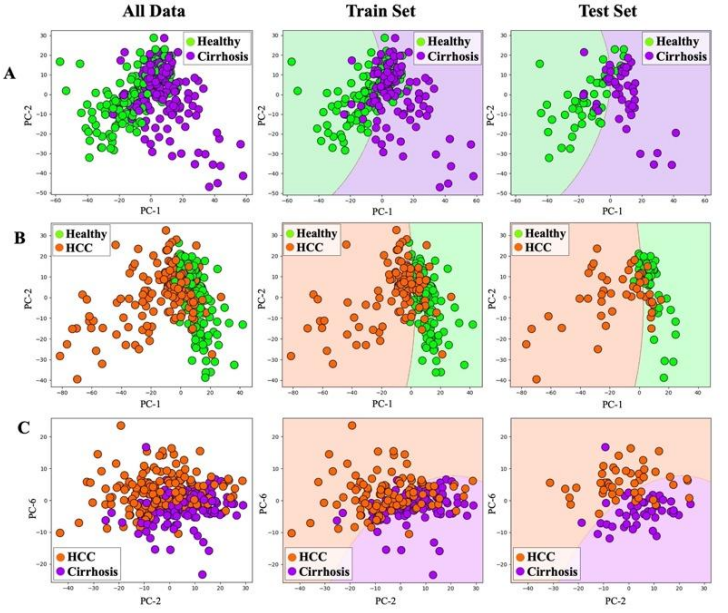

Fig. 3: Scatter plots for the diagnostic differentiation by PCA-SVM between cirrhosis, HCC, and healthy groups using 2 principal components (PCs) A. Cirrhosis vs. Healthy; B. HCC vs. Healthy; C. Cirrhosis vs. HCC.

suggests an elevation in collagen levels in cirrhotic and HCC patients, aligning well with previous studies,[54–56] which noted significantly higher serum type IV collagen levels in patients with cirrhosis and liver cancer, including HCC and metastatic liver cancer, compared to healthy controls. This increase is linked to the tumor microenvironment and hepatic fibroplasia, both of which play critical roles in the progression and prognosis of liver cancer.[54] Consequently, the type IV collagen level in liver disease patients has become a valuable serological biomarker for the diagnosis and prognosis of early-stage liver fibrosis,[56] indicating the extent of hepatic fibrosis and tumor growth. Notably, the clear spectral distinction of the collagen peak in the amide III band in serum Raman spectra between HCC and cirrhosis groups compared to the healthy group suggests that this peak could be a valuable Raman marker for monitoring and identifying the progression of liver fibrosis and assessing the severity of liver disease. Therefore, our findings highlight the potential of Raman spectroscopy as a rapid and label-free method that could be effectively used to observe these biomolecular changes in collagen levels through the analysis of this specific Raman marker band in the amide III region, providing a promising tool for monitoring the progression of liver disease.

Moreover, compared to healthy subjects, a significant increase in the levels of aromatic amino acids (AAAs) was found in patients with HCC and cirrhosis. This increase was observed in tryptophan (757 and 878 cm^{-1}), tyrosine (831 and 853 cm^{-1}), and phenylalanine (1004 cm^{-1}). The elevated concentration of AAAs in the serum of patients with advanced and chronic liver disease is attributed to the impaired metabolic oxidation involved in protein synthesis.[42] This abnormal amino acid metabolism has been linked to liver disease and the occurrence of HCC in patients. Cancer cells have a greater need for amino acids for protein synthesis, providing the energy necessary for tumor cell development and malignancy.[57,58] The increase in AAAs in serum was found to be indicative of progressive liver disease and the occurrence of cirrhosis-related complications, such as encephalitis.[59] Therefore, the increased AAA serum levels observed in patients with HCC and cirrhosis align well with existing medical findings and suggest that Raman spectroscopy could be a valuable tool for detecting these biomolecular changes.

In addition, a significantly higher serum cholesterol level (548 and 699 cm^{-1}) was found in HCC patients compared to cirrhosis and healthy individuals. HCC has been associated with altered cholesterol metabolism. In patients with HCC, there is a tendency towards hypercholesterolemia, particularly in advanced stages of the disease. This is often associated with metabolic syndrome and dyslipidemia, which are risk factors for HCC.[60] The presence of hypercholesterolemia in HCC has been linked to the regulation of PCSK9, a protein that influences LDL cholesterol levels. High glucose levels can increase PCSK9 expression, contributing to elevated LDL cholesterol in HCC patients.[61]

In contrast, the serum levels of β-carotene (1157 and 1527 cm^{-1}) were significantly lower in cirrhotic and HCC patients compared to healthy controls. This reduction in serum β-carotene has been reported in cirrhosis,[62] non-alcoholic steatohepatitis (NASH),[63] cholangiocarcinoma,[24] colorectal cancer,[64] and nasopharyngeal cancer.[65] A significant downward trend in serum β-carotene concentrations was observed with increasing hepatic fibrosis stage, with significantly lower levels in patients with hepatitis C virus (HCV) and cirrhosis compared to healthy controls.[62] β-carotene is known for its capacity to inhibit free radicals, thereby protecting cellular membranes, DNA, and reactive oxygen species from oxidative damage; thus, a decrease in

Table 3: Classification performance of the PCA–SVM model across validation strategies for cirrhosis, HCC, and healthy groups.

Validation Strategy	Group	Cross-validated diagnostic performance (%)			AUC of ROC curves
		Sensitivity	Specificity	Accuracy	
5-fold subject-wise CV	Cirrhosis-Healthy	84.7	94.0	89.3	0.951
	HCC-Healthy	90.0	95.3	92.7	0.980
	Cirrhosis-HCC	83.3	90.00	93.5	0.929
Leave-One Subject-Out (LOSO) CV	Cirrhosis-Healthy	83.3	94.7	89.0	0.952
	HCC-Healthy	92.0	95.3	93.7	0.977
	Cirrhosis-HCC	84.0	89.3	86.7	0.930

serum β-carotene may indicate cellular membrane damage and a reduction in antioxidant activity, which has potential implications for cancer prevention.[66] The liver is integral to carotenoid metabolism and serves as the primary storage organ for β-carotene.[67,68] High carotenoid intake has been recognized as providing an essential antioxidant benefit, associated with a reduction in cancer mortality by boosting the immune system.[69] Thus, as liver disease progresses, β-carotene levels typically decline, indicating lower serum β-carotene concentrations in patients with advanced liver disease.[62] Therefore, monitoring serum β-carotene levels in liver disease patients can provide valuable insights into disease progression, and Raman spectroscopy presents a simple, label-free, and effective technique for this task.

To further improve the diagnostic capacity of our approach, Raman spectral analysis was combined with a machine learning method to classify cirrhosis, HCC, and healthy groups. The spectral data were first dimensionally reduced by principal component analysis (PCA), which transformed the data into principal components (PCs) based on extracted spectral features. These PCs captured the most variance in the original dataset, thus representing the key characteristics of the spectral signatures. The scores of the selected PCs were then used as input features for a support vector machine (SVM) algorithm to perform supervised classification, distinguishing between cirrhosis-healthy, HCC-healthy, and cirrhosis-HCC groups.

Pairwise classification results are visualized in Fig. 3, where scatter plots of the two PCs illustrate group separation. Fig. 3A shows that, despite cirrhosis samples exhibiting broader variability compared to the tightly clustered healthy group, the classifier still achieved a meaningful decision boundary. This is particularly notable given that over 90% of cirrhosis cases were classified as Child–Pugh A, representing early-stage disease. The ability to distinguish these early cirrhotic cases from healthy individuals demonstrates the sensitivity of Raman-derived spectral features in detecting incipient liver dysfunction. In Fig. 3B, the separation between healthy and HCC groups is more clearly defined, reflecting the pronounced molecular alterations associated with hepatocarcinogenesis. Notably, the separation also captured early to intermediate HCC, with 67% of patients staged as BCLC A–B, highlighting the algorithm's capacity to detect malignancy during clinically actionable phases. Meanwhile, Fig. 3C shows a more subtle distinction between cirrhosis and HCC, which is expected due to overlapping biochemical profiles during early disease progression. Nevertheless, the method still achieved reliable classification, indicating its potential utility in challenging diagnostic scenarios where conventional biomarkers may be insufficient.

To rigorously assess generalizability while mitigating overfitting, the number of PCs was increased from 2 to 30. Two subject-wise validation strategies were employed: five-fold subject-wise cross-validation using Group K Fold and leave-one-subject-out (LOSO) cross-validation. The 5-fold subject-wise cross-validation (5-fold CV) balances computational efficiency with model generalization assessment. Through subject-level separation across folds**,** it prevents data leakage and is well-suited for evaluating models on medical datasets.[70] LOSO-CV is particularly suited for biomedical spectroscopy studies with repeated measures from each subject, as it simulates real-world deployment by testing the system on entirely unseen individual.[71,72] This method minimizes data leakage and provides a robust estimate of the discriminative capacity of the approach. Both strategies ensured that samples from the same subject were never present in both training and test sets.

As summarized in Table 3, the healthy–HCC differentiation achieved the highest accuracy (92.7% 5-fold CV; 93.7% LOSO-CV), reflecting the distinct spectral differences between non-diseased and cancerous states. Notably, this predictive strength was maintained despite the dataset being dominated by initial and intermediate HCC cases, underscoring the approach's potential for early cancer detection. The cirrhosis–HCC differentiation also demonstrated strong outcomes, with accuracies of 93.5% (5-fold CV) and 86.7% (LOSO-CV), despite the close biological connection between these conditions. This result highlights the method's capacity to detect intricate spectral shifts associated with malignant transformation in cirrhotic patients. Lastly, the cirrhosis–healthy comparison showed consistent diagnostic effectiveness, with accuracies of 89.3%(5-fold CV)

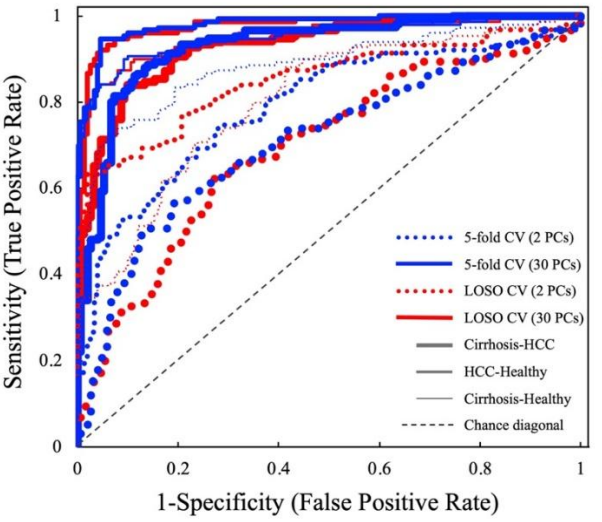

Group	AUC of ROC curves			
	5-fold subject-wise CV		Leave-One-Subject-Out (LOSO) CV	
	2 PCs	30 PCs	2 PCs	30 PCs
Cirrhosis-Healthy	0.884	0.951	0.803	0.952
HCC-Healthy	0.789	0.98	0.851	0.977
Cirrhosis-HCC	0.71	0.929	0.692	0.93

Fig. 4: Cross-validated ROC curves for the PCA-SVM classification distinguishing among liver cirrhosis, hepatocellular carcinoma, and healthy groups. The figure compares models using 2 principal components (PCs; dotted lines) versus 30 PCs (solid lines). Blue lines indicate 5-fold cross-validation, while red lines represent leave-one-subject-out (LOSO) cross-validation. Line thickness corresponds to group comparisons: thin for cirrhosis vs. healthy, medium for HCC vs. healthy, and thick for cirrhosis vs. HCC.

and 89.0% (LOSO-CV). This pair posed a more complex group separation task compared to the others, primarily due to the predominance of early-stage cirrhosis in the dataset. Such cases often exhibit biomolecular profiles that closely resemble those of healthy individuals, resulting in a degree of spectral overlap. Nonetheless, the algorithm still achieved over 83.0% sensitivity and specificity, emphasizing its potential for detecting early liver dysfunction with clinically meaningful accuracy.

Fig. 4 further compares ROC curves of models using 2 PCs and 30 PCs. Using only 2 PCs resulted in moderate predictive outcomes (AUC: 0.692–0.884), whereas incorporating 30 PCs significantly improved differentiation approach accuracy, with AUCs reaching 0.929–0.980 across all pairs. The ROC curves of the 30-PC models consistently approached the top-left corner, indicating higher true positive rates and lower false positive rates. This improvement can be attributed to the inclusion of a more comprehensive set of Raman spectral features, thereby enabling the model to capture and discern more nuanced data patterns present within the spectra. More PCs can effectively capture variance in high-dimensional datasets, such as spectral data, which is critical for optimizing the performance of machine learning models.[73] However, including too many PCs may introduce noise and irrelevant variation, potentially leading to overfitting. To address this, rigorous subject-wise validation methods were employed to ensure robust performance assessment and minimize overfitting. These techniques evaluate discriminative power across independent data subsets, thereby enhancing the model's reliability and generalizability.

Following feature extraction and validation, machine learning was employed to simultaneously classify serum samples from healthy individuals, cirrhosis patients, and HCC patients, as shown in Fig. 5A-E. In Fig. 5A, PCA projection onto the first two components reveals that cirrhotic samples partially overlap with both healthy and HCC groups, highlighting their transitional nature and the shared molecular signatures observed in early-stage disease. In contrast, HCC samples form a distinct cluster along the positive PC1 axis, reflecting pronounced spectral shifts associated with malignancy. Fig. 5B presents the PCA-SVM decision boundaries based on the same two components, with separate visualizations for the train and test sets. In the train set, the data distribution illustrates a biological continuum between cirrhosis and HCC. In the test set, healthy and cirrhotic samples appear partially overlapping; however, no instance from either group was misclassified as HCC. Nevertheless, this 2D scatterplot provides a simplified view of how the model separates the groups but does not fully capture the complexity of the classification task.

To better distinguish subtle differences-especially between healthy and cirrhotic profiles—additional features were needed. While 30 principal components were sufficient for earlier binary classification tasks, this multiclass diagnostic setting required a broader feature space. Therefore, the feature set was expanded to 50 PCs, capturing 99.0% of the cumulative variance. This allowed the model to leverage both dominant Raman spectral trends and more nuanced clinical signatures, ultimately improving its classification accuracy and robustness. Fig. 5C and 5D present confusion matrices from the multiclass classification analysis based on dimensionally reduced data. By utilizing this enriched feature space, the model delivered consistent and strong performance across both subject-wise validation approaches. Overall accuracies reached 85.9% in 5-fold CV and 85.3% in LOSO-CV, with class-wise accuracies exceeding 80% across all diagnostic categories. The highest accuracy was achieved in HCC detection (93.3%, 5-fold CV), underscoring its

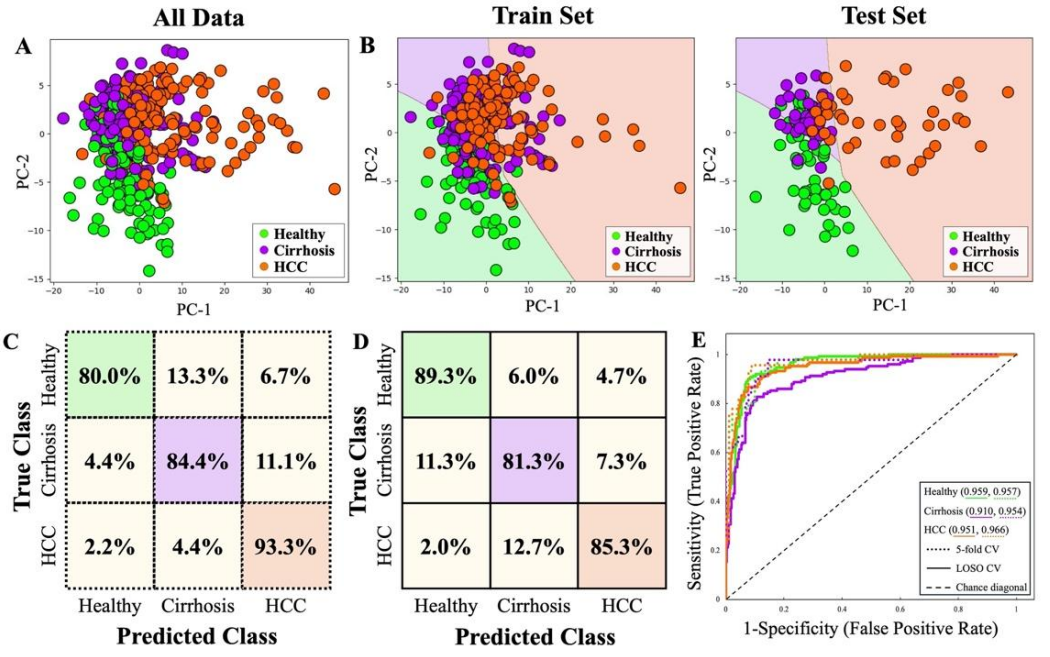

Fig. 5: The PCA-SVM classification among sera of healthy subjects, cirrhosis patients, and HCC patients. A. PCA scatter plot of 2 principal components (PCs) displaying all data for each of the three groups. B. SVM classification analysis for both the training set (left) and test set (right). C–D. Confusion matrices generated using the top 50 PCs for classification: C from 5-fold subject-wise cross-validation, and D from leave-one-subject-out (LOSO) cross-validation. E. Receiver operating characteristic (ROC) curves corresponding to the classification results in C and D, illustrating model performance for each class under both validation strategies.

diagnostic reliability. The ROC curves in Fig. 5E further validate the model's high classification precision, with AUC values exceeding 0.90 for all comparisons. Importantly, this approach supports direct three-class prediction within a single framework. It facilitates rapid and objective decision-making in clinical contexts where accurate differentiation between healthy individuals, cirrhotic patients, and those with HCC is critical for early diagnosis and treatment planning.

To contextualize these findings, the performance of Raman–ML was compared against widely used diagnostic tools, as summarized in Table 4. Each technique presents a trade-off between sensitivity and specificity, influenced by both methodological limitations and clinical context. Imaging modalities such as ultrasound, CT, and MRI are commonly employed. Ultrasound performs well in detecting cirrhosis but is less effective for identifying HCC, especially in obese patients.[74] CT and MRI offer enhanced precision for detecting HCC, but their use is often limited by high costs and the need for contrast agents or advanced imaging protocols to achieve optimal accuracy.[75] Liver biopsy remains the reference standard due to its diagnostic reliability; however, its invasive nature and risks—such as bleeding and sampling error—restrict its suitability for routine clinical application.[76] Noninvasive scoring systems like FIB-4 and APRI serve as more accessible alternatives. APRI generally outperformsFIB-4, though both exhibit limited clinical evaluation capability in early-stage disease or specific patient subgroups.[77] Serum biomarkers—AFP and PIVKA-II—demonstrate inconsistent reliability. PIVKA-II provides higher specificity but lower sensitivity in distinguishing HCC from cirrhosis. Their diagnostic predictive power is highly dependent on disease stage, comorbidities, and the choice of cutoff values.[78] Lower thresholds improve sensitivity but raise the likelihood of false positives, whereas higher thresholds enhance specificity at the cost of missing early-stage disease.[79] Critically, no current blood-based biomarker strategy is capable of simultaneously distinguishing healthy individuals, cirrhosis patients, and HCC patients with sufficient reliability. Most existing approaches are optimized for binary categorization or are designed to detect a single condition. This underscores the need for a more comprehensive and noninvasive screening solution that can differentiate across multiple liver disease stages within a unified diagnostic platform.

The proposed method in this study—Raman spectroscopy combined with machine learning (Raman–ML)—offers a powerful alternative. It demonstrated consistent performance across all pairwise comparisons: 83.3% sensitivity and 94.7% specificity for cirrhosis vs. healthy, 92.0% sensitivity and 95.3% specificity for HCC vs. healthy, and 84.0% sensitivity and 89.3% specificity for HCC vs. cirrhosis. Remarkably, it is the only tool in this comparison capable of enabling simultaneous three-way classification in a single step—an advantage that simplifies clinical interpretation and supports early detection across the disease spectrum. Its affordability, minimally-invasive nature, and independence from biomarker cut-off thresholds make it particularly suitable for point-of-care use, especially in resource-constrained settings. By leveraging the full Raman spectral signature rather than relying on

Table 4: Comparative diagnostic performance of various methods for cirrhosis and HCC groups.

Categories	Techniques	Cirrhosis–Healthy		HCC–Healthy		HCC–Cirrhosis		Cost per Test (USD)	Limitations
		Sensitivity (%)	Specificity (%)	Sensitivity (%)	Specificity (%)	Sensitivity (%)	Specificity (%)		
1. Imaging Techniques	Ultrasound	91[80]	94[80]	40–81 [81]	80–100 [81]	43.9-84 [82,83]	91.5[83]	100–300	- Limited ability to detect small or isoechoic lesions; accuracy depends on operator skill.[84] - Reduced sensitivity in obese patients or those with fatty liver.[84] - Expensive - Potential for misdiagnosis due to overlapping imaging features.[75]
	CT scan	—	—	84[85]	99[85]	73.3 [86]	77.5[86]	500–1,500	- Limited ability to differentiate lesions with similar appearances, such as hemangiomas and focal nodular hyperplasia (FNH).[75]
	MRI	—	—	84[87]	94[87]	87.3[88]	81.6[88]	1,000–3,000	-Challenges remain in distinguishing lesions with similar imaging characteristics.[75] -Often requires advanced imaging techniques or contrast agents to improve diagnostic accuracy.[75]
	Elastography	81[89]	88[89]	—	—	—	—	-Fibro Scan: 100–300 per scan, -Magnetic Resonance Elastography (MRE): 1,000–2,500	-Inaccurate in patients with inflammation, congestion, or obesity.[90] -Operator skill and patient cooperation affect results.[90] -Not specific for fibrosis due to cirrhosis only.[90]
2. Liver Biopsy	Liver Biopsy	—	—	66-93[91]	100[91]	85.1[92]	100[92]	1,000–3,000	-Invasive with risk of bleeding and sampling error.[76] -Cannot represent whole liver. -Not suitable for routine or repeated use.[76]
3. Clinical scoring	Fibrosis-4 Index (FIB-4)	41.3[77]	91.0[77]	—	—	—	—	<20	-Limited specificity and sensitivity, especially in

Categories	Techniques	Cirrhosis–Healthy		HCC–Healthy		HCC–Cirrhosis		Cost per Test (USD)	Limitations
		Sensitivity (%)	Specificity (%)	Sensitivity (%)	Specificity (%)	Sensitivity (%)	Specificity (%)		
systems	AST to Platelet Ratio Index (APRI)	93[77]	98.8[77]	—	—	—	—	<20	intermediate fibrosis stages.[77] -Influenced by comorbidities and lab variability.[77] -Low sensitivity for early-stage HCC.
4. Serum Biomarkers	Alpha-Fetoprotein (AFP)	—	—	32-61[79]	86-99[79]	65.9[83]	90.5[83]	30–100	-Cut-off variability affects sensitivity and specificity.[79] -False positives in patients with chronic liver disease or cirrhosis.[93] -Elevated levels can also occur in non-malignant liver disease.[97]
	Protein Induced by Vitamin K Absence or Antagonist-II (PIVKA-II)	—	—	58.3[94]	92.6[94]	48-62 [95,96]	81-98 [95,96]	50–150	-Diagnostic accuracy is influenced by underlying etiology and comorbidities.[97] -Diagnostic accuracy depends on selected cut-off.[78] -Low sensitivity between cirrhosis and HCC differentiation. [97] -Generalizability across populations is uncertain.
5. This study	Raman + ML	83.3	94.7	92.0	95.3	84.0	89.3	10	-Long-term stability of the model. -Limited sample size may affect model accuracy and validation.

predefined biomarkers, the method captures molecular variations that conventional strategies may overlook. These strengths highlight Raman–ML as a practical and scalable diagnostic platform with strong potential for integration into liver disease screening workflows.

To enhance generalizability and long-term clinical relevance, future investigations should include external validation across diverse populations and incorporate longitudinal monitoring. This includes expanding the sample pool to cover a broader range of racial, gender, and age groups. Such demographic diversification could enhance the robustness, fairness, and external validity of the proposed diagnostic framework. Of interest, age diversity is a critical consideration, as a recent study showed that 20.2% of cirrhosis patients were young adults aged 18–40 years—a proportion significantly higher than those reported in prior studies from other tertiary care centers.[98] This emerging trend highlights a shifting age demographic and emphasizes the importance of investigating younger populations. To address this, future studies should incorporate a broader age spectrum, with particular focus on early-stage disease in younger adults. These insights may inform the development of age-specific screening and intervention strategies, ultimately promote early diagnosis and improve patient outcomes.

To enhance generalizability and long-term clinical relevance, future investigations should include external validation across diverse populations and incorporate longitudinal monitoring. This includes expanding the sample pool to cover a broader

range of racial, gender, and age groups. Such demographic diversification could enhance the robustness, fairness, and external validity of the proposed diagnostic framework. Of interest, age diversity is a critical consideration, as a recent study showed that 20.2% of cirrhosis patients were young adults aged 18–40 years—a proportion significantly higher than those reported in prior studies from other tertiary care centers.[98] This emerging trend highlights a shifting age demographic and emphasizes the importance of investigating younger populations. To address this, future studies should incorporate a broader age spectrum, with particular focus on early-stage disease in younger adults. These insights may inform the development of age-specific screening and intervention strategies, ultimately promote early diagnosis and improve patient outcomes.

In addition to demographic considerations, maintaining the long-term stability of diagnostic accuracy is also essential for real-world deployment. This requires continuous evaluation using newly acquired samples, as various factors—such as aging, disease progression, and environmental influences—can affect system reliability over time. Several studies have shown that protein expression profiles evolve with age and correlate with metabolic shifts, thus reflecting both physiological and pathological transformations.[99,100] Additional factors such as diet, personalized medicine, and environmental exposures further shape the human proteome.[101,102] This biological variability poses a challenge to maintaining consistency, as features learned at one time point may behave differently in future datasets or across populations. Consequently, algorithms trained exclusively on cross-sectional data may fail to generalize to real-world scenarios that evolve over time. Recent reports have confirmed that performance degradation is a well-recognized issue in clinical machine learning deployments, particularly due to data drift and shifting medical practices. A previous study demonstrated that deployed approaches required retraining approximately every three months during periods of significant clinical change.[103] To mitigate this, model updates should be driven by performance monitoring rather than fixed time intervals. Retraining is best initiated once a measurable decline in performance is detected.[104] Therefore, future work should include the development of a prospective monitoring framework and the implementation of incremental retraining strategies. Together, these measures reinforce the role of this approach as a reliable component within clinical deployment strategies.

In conclusion, this study demonstrates a simple, rapid, yet effective approach by integrating conventional Raman spectroscopy (RS) with machine learning for simultaneous serum-based detection and classification of HCC, liver cirrhosis, and healthy individuals. It addresses the need for a quick and uncomplicated screening technique to distinguish these two liver disease types from healthy subjects. Unlike surface-enhanced Raman spectroscopy (SERS), conventional RS is simpler and does not require complex Raman-enhancing metallic nanoparticles, which can add extra costs and require intricate fabrication processes. Although there are concerns regarding the sensitivity of conventional RS compared to SERS, this study shows that RS, when combined with machine learning, can enhance diagnostic capabilities, achieving substantial sensitivity, specificity, and accuracy in detecting and differentiating the liver disease types and healthy controls. Moreover, RS alone can provide spectral information and significant marker bands that are useful for monitoring liver disease progression without concerns about the interaction of metallic nanoparticles with biological samples as in the case of SERS. Therefore, RS coupled with machine learning offers a promising strategy as an effective diagnostic tool, potentially useful for cirrhosis and HCC screening, particularly in low-resource settings. It has the potential to complement existing imaging techniques, thereby improving clinical diagnosis, prognosis, and patient outcomes for cirrhosis and HCC, ultimately helping to reduce the global burden of liver disease.

4. Conclusion

This study developed an optics-based diagnostic method using Raman spectroscopy coupled with supervised machine learning analysis for the rapid, serum-based differentiation between HCC, cirrhosis, and healthy individuals. The study revealed several Raman characteristic peaks that indicated significant biomolecular differences between the three groups. In particular, the amide III band of collagen at approximately 1246 cm^{-1} could be used as a Raman marker band to separate HCC and cirrhosis from healthy individuals due to the distinct separation of the Raman feature. The serum levels of collagen, aromatic amino acids, and cholesterol were found to be significantly higher in the cirrhosis and HCC patients than in the healthy controls, whereas β-carotene was significantly lower in the cirrhosis and HCC groups. The diagnostic potential of Raman spectroscopy was evidently improved with the aid of a machine-learning algorithm. The classification analysis of the Raman spectra using the PCA-SVM model demonstrated strong diagnostic performance in differentiating between cirrhosis and HCC. The 5-fold subject-wise cross-validation achieved 83.3% sensitivity, 90.0% specificity, and 93.5% accuracy. Similarly, leave-one-subject-out (LOSO) cross-validation produced comparable results with 84.0% sensitivity, 89.3% specificity, and 86.7% accuracy. The simultaneous differential diagnosis between the three groups showed that each group could be correctly identified by PCA-SVM with the LOSO-CV approach yielded accuracies of 89.3% for healthy individuals, 81.3% for cirrhosis, and 85.3% for HCC. This approach demonstrated high discriminative performance in separating early cirrhosis from early to intermediate HCC, which constituted the majority of clinical samples. This highlights the potential of Raman-based classification as a sensitive tool for detecting subtle molecular alterations prior to advanced disease progression, thereby supporting its use in early detection and surveillance strategies. Thus, this rapid serum-based technique could be

applied to screening healthy individuals who are at risk of developing cirrhosis or cirrhosis patients who are at risk of progressing to HCC. It addresses several diagnostic challenges associated with current methods for diagnosing liver cirrhosis and HCC, particularly the inadequacies and limited diagnostic capacity of current blood biomarker tests, such as alpha-fetoprotein (AFP), as well as the limitations of existing imaging modalities, especially in resource-constrained settings. By proposing an optics-based, machine learning-enhanced diagnostic strategy, this study offers a rapid, simple, and cost-effective alternative and complement to existing techniques for the detection and diagnosis of these liver disease conditions, with the potential to improve patient outcomes.

Acknowledgments

This study was supported by the Fundamental Fund of Khon Kaen University from the National Science, Research and Innovation Fund (NSRF), Thailand (fiscal year 2024). We express our gratitude to the Faculty of Medicine at Khon Kaen University for providing access to the Horiba XploRA PLUS confocal Raman microscope, which was used for data collection. We also thank Asst. Prof. Chavis Srichan for his advice on machine learning algorithms and Ms. Kodchakorn Khemtonglang for her assistance during the research study.

Conflict of Interest

There is no conflict of interest.

Supporting Information

Not applicable.

CRediT Statement

Sasikan Borwornmote: Data curation, Formal analysis, Investigation, Methodology, Software, Validation, Visualization, Writing – original draft, Writing – review & editing; **Peeraya Suksuratin:** Data curation, Formal analysis, Investigation, Methodology; **Rutchanee Rodpai:** Data curation, Methodology, Resources, Validation; **Wattana Sukeepaisarnjaroen:** Conceptualization, Resources, Validation; **Pewpan M. Intapan:** Conceptualization, Methodology, Resources, Validation, Writing – review & editing; **Wanchai Maleewong:** Conceptualization, Methodology, Resources, Validation, Writing – review & editing; **Oranat Chuchuen:** Conceptualization, Formal analysis, Funding acquisition, Methodology, Project administration, Resources, Supervision, Validation, Writing – original draft, Writing – review & editing.

References

[1] Z. Dong, Y. Wang, W. Jin, Liver cirrhosis: molecular mechanisms and therapeutic interventions, *MedComm*, 2024, **5**, e721, doi: 10.1002/mco2.721.

[2] X.-N. Wu, F. Xue, N. Zhang, W. Zhang, J.-J. Hou, Y. Lv, J.-X. Xiang, X.-F. Zhang, Global burden of liver cirrhosis and other chronic liver diseases caused by specific etiologies from 1990 to 2019, *BMC Public Health*, 2024, **24**, 363, doi: 10.1186/s12889-024-17948-6.

[3] E.K.J. Tham, D.J.H. Tan, P. Danpanichkul, C.H. Ng, N. Syn, B. Koh, *et al.*, The Global Burden of Cirrhosis and Other Chronic Liver Diseases in 2021, *Liver international: official journal of the International Association for the Study of the Liver*, Liver Int, 2025, **45**, doi: 10.1111/LIV.70001.

[4] H. Devarbhavi, S. K. Asrani, J. P. Arab, Y. A. Nartey, E. Pose, P. S. Kamath, Global burden of liver disease: 2023 update, *Journal of Hepatology*, 2023, **79**, 516-537, doi: 10.1016/j.jhep.2023.03.017.

[5] D. Gabbia, S. De Martin, Insights into hepatocellular carcinoma: from pathophysiology to novel therapies, *International Journal of Molecular Sciences*, 2024, **25**, 4188, doi: 10.3390/ijms25084188.

[6] Q. Guo, X. Zhu, N. M. Beeraka, R. Zhao, S. Li, F. Li, P. A. Mahesh, V. N. Nikolenko, R. Fan, J. Liu, Projected epidemiological trends and burden of liver cancer by 2040 based on GBD, CI5plus, and WHO data, *Scientific Reports*, 2024, **14**, 28131, doi: 10.1038/s41598-024-77658-2.

[7] L. M. Cruz-Rodríguez, A. G. Pérez-Castañeda, J. I. Cervantes-Contreras, E. S. García-Jiménez, J. M. Aldana-Ledesma, J. A. V. Velasco, Clinical and epidemiological characterization of patients with hepatocarcinoma, *Annals of Hepatology*, 2024, **29**, 101427, doi: 10.1016/j.aohep.2024.101427.

[8] A. Quaglia, Hepatocellular carcinoma: a review of diagnostic challenges for the pathologist, *Journal of Hepatocellular Carcinoma*, Dove Medical Press Ltd., 2018, **5**, 99–108, doi: 10.2147/jhc.s159808.

[9] H. Hanif, M. J. Ali, A. T. Susheela, I. W. Khan, M. A. Luna-Cuadros, M. M. Khan, D. T. Lau, Update on the applications and limitations of alpha-fetoprotein for hepatocellular carcinoma, *World Journal of Gastroenterology*, 2022, **28**, 216-229, doi: 10.3748/wjg.v28.i2.216.

[10] S. An, X. Zhan, M. Liu, L. Li, J. Wu, Diagnostic and prognostic nomograms for hepatocellular carcinoma based on PIVKA-II and serum biomarkers, *Diagnostics*, 2023, **13**, 1442, doi: 10.3390/diagnostics13081442.

[11] D. Y. Kim, B. N. Toan, C. K. Tan, I. Hasan, L. Setiawan, M. L. Yu, N. Izumi, N. N. Huyen, P. K. Chow, R. Mohamed, S. L. Chan, T. Tanwandee, T. Y. Lee, T. T. N. Hai, T. Yang, W. C. Lee, H. L. Y. Chan, Utility of combining PIVKA-II and AFP in the surveillance and monitoring of hepatocellular carcinoma in the Asia-Pacific region, *Clinical and Molecular Hepatology*, 2023, **29**, 277-292, doi: 10.3350/cmh.2022.0212.

[12] A. Sangiovanni, M. A. Manini, M. Iavarone, R. Romeo, L. V. Forzenigo, M. Fraquelli, S. Massironi, C. Della Corte, G. Ronchi, M. G. Rumi, P. Biondetti, M. Colombo, The diagnostic and economic impact of contrast imaging techniques in the diagnosis of small hepatocellular carcinoma in cirrhosis, *Gut*,

2010, **59**, 638-644, doi: 10.1136/gut.2009.187286.
[13] C. Nicolau, R. Vilana, C. Brú, The use of contrast-enhanced ultrasound in the management of the cirrhotic patient and for detection of HCC, *European Radiology*, 2004, **14**, P63-P71, doi: 10.1007/s10406-004-0080-7.
[14] E. Turko, Radiological imaging in liver tumors: diagnosis and management strategies. *The Radiology of Cancer*, Istanbul: Nobel Tip Kitabevleri, 2024, 161-183, doi: 10.69860/nobel.9786053359364.14.
[15] O. Chuchuen, M. H. Henderson, C. Sykes, M. S. Kim, A. D. Kashuba, D. F. Katz, Quantitative analysis of microbicide concentrations in fluids, gels and tissues using confocal Raman spectroscopy, *PLoS One*, 2013, **8**, e85124, doi: 10.1371/journal.pone.0085124.
[16] O. Chuchuen, J. R. Maher, M. G. Simons, J. J. Peters, A. P. Wax, D. F. Katz, Label-free measurements of tenofovir diffusion coefficients in a microbicide gel using Raman spectroscopy, *Journal of Pharmaceutical Sciences*, 2017, **106**, 639-644, doi: 10.1016/j.xphs.2016.09.030.
[17] O. Chuchuen, J. R. Maher, M. H. Henderson, M. Desoto, L. C. Rohan, A. Wax, D. F. Katz, Label-free analysis of tenofovir delivery to vaginal tissue using co-registered confocal Raman spectroscopy and optical coherence tomography, *PLoS One*, 2017, **12**, e0185633, doi: 10.1371/journal.pone.0185633.
[18] O. Chuchuen, R. Madee, J. Paluka, C. Lapjit, P. M. Intapan, Rapid quantitative detection of cannabinoids using laser Raman spectroscopy, *Engineering, Technology & Applied Science Research*, 2024, **14**, 16998-17004, doi: 10.48084/etasr.8203.
[19] O. Chuchuen, T. Thammaratana, O. Sanpool, R. Rodpai, W. Maleewong, P. M. Intapan, Rapid label-free analysis of Opisthorchis viverrini eggs in fecal specimens using confocal Raman spectroscopy, *PLoS One*, 2019, **14**, e0226762, doi: 10.1371/journal.pone.0226762.
[20] G. Satpathy, C. G. K., K. Elayaraja, M. D. R, A. Subramania, Z. Guo, S. Umapathy, E. Manikandan, Nanoparticles and bacterial interaction of host-pathogens and the detection enhancement of biomolecules by fluorescence Raman spectroscopic investigation, *Engineered Science*, 2022, **20**, 341–351, doi: 10.30919/es8d767.
[21] K. J. I. Ember, M. A. Hoeve, S. L. McAughtrie, M. S. Bergholt, B. J. Dwyer, M. M. Stevens, K. Faulds, S. J. Forbes, C. J. Campbell, Raman spectroscopy and regenerative medicine: a review, *NPJ Regenerative Medicine*, 2017, **2**, 12, doi: 10.1038/s41536-017-0014-3.
[22] K. Hanna, E. Krzoska, A. M. Shaaban, D. Muirhead, R. Abu-Eid, V. Speirs, Raman spectroscopy: current applications in breast cancer diagnosis, challenges and future prospects, *British Journal of Cancer*, 2022, **126**, 1125-1139, doi: 10.1038/s41416-021-01659-5.
[23] M.-J. Jeng, M. Sharma, L. Sharma, T.-Y. Chao, S.-F. Huang, L.-B. Chang, S.-L. Wu, L. Chow, Raman spectroscopy analysis for optical diagnosis of oral cancer detection, *Journal of Clinical Medicine*, 2019, **8**, 1313, doi: 10.3390/jcm8091313.
[24] P. Suksuratin, R. Rodpai, V. Luvira, P. M. Intapan, W. Maleewong, O. Chuchuen, Rapid label-free detection of cholangiocarcinoma from human serum using Raman spectroscopy, *PLoS One*, 2022, **17**, e0275362, doi: 10.1371/journal.pone.0275362.
[25] E. Gurian, P. Giraudi, N. Rosso, C. Tiribelli, D. Bonazza, F. Zanconati, M. Giuricin, S. Palmisano, N. de Manzini, V. Sergo, A. Bonifacio, Differentiation between stages of non-alcoholic fatty liver diseases using surface-enhanced Raman spectroscopy, *Analytica Chimica Acta*, 2020, **1110**, 190-198, doi: 10.1016/j.aca.2020.02.040.
[26] G. Lü, X. Zheng, X. Lü, P. Chen, G. Wu, H. Wen, Label-free detection of echinococcosis and liver cirrhosis based on serum Raman spectroscopy combined with multivariate analysis, *Photodiagnosis and Photodynamic Therapy*, 2021, **33**, 102164, doi: 10.1016/j.pdpdt.2020.102164.
[27] I. Taleb, G. Thiéfin, C. Gobinet, V. Untereiner, B. Bernard-Chabert, A. Heurgué, C. Truntzer, P. Hillon, M. Manfait, P. Ducoroy, G. D. Sockalingum, Diagnosis of hepatocellular carcinoma in cirrhotic patients: a proof-of-concept study using serum micro-Raman spectroscopy, *The Analyst*, 2013, **138**, 4006-4014, doi: 10.1039/c3an00245d.
[28] Q. Ou, X. Yang, W. Yang, L. Jiang, K. Qian, Y.-M. Shi, G. Liu, Based on serum Raman and fluorescence spectra to diagnose liver cancer, *Research Square*, 2022, doi: 10.21203/rs.3.rs-1118522/v1.
[29] T. Tolstik, C. Marquardt, C. Beleites, C. Matthäus, C. Bielecki, M. Bürger, C. Krafft, O. Dirsch, U. Settmacher, J. Popp, A. Stallmach, Classification and prediction of HCC tissues by Raman imaging with identification of fatty acids as potential lipid biomarkers, *Journal of Cancer Research and Clinical Oncology*, 2015, **141**, 407-418, doi: 10.1007/s00432-014-1818-9.
[30] X. Li, T. Yang, S. Li, L. Jin, D. Wang, D. Guan, J. Ding, Noninvasive liver diseases detection based on serum surface enhanced Raman spectroscopy and statistical analysis, *Optics Express*, 2015, **23**, 18361-18372, doi: 10.1364/OE.23.018361.
[31] D.-B. Grys, R. Chikkaraddy, M. Kamp, O. A. Scherman, J. J. Baumberg, B. de Nijs, Eliminating irreproducibility in SERS substrates, *Journal of Raman Spectroscopy*, 2021, **52**, 412-419, doi: 10.1002/jrs.6008.
[32] S. S. Panikar, D. Cialla-May, E. De la Rosa, P. Salas, J. Popp, Towards translation of surface-enhanced Raman spectroscopy (SERS) to clinical practice: Progress and trends, *TrAC Trends in Analytical Chemistry*, 2021, **134**, 116122, doi: 10.1016/j.trac.2020.116122.
[33] J. Houston, F. G. Glavin, M. G. Madden, Robust classification of high-dimensional spectroscopy data using deep learning and data synthesis, *Journal of Chemical Information and Modeling*, 2020, **60**, 1936-1954, doi: 10.1021/acs.jcim.9b01037.
[34] A. Sheoran, R. Boora, M. Jangra, C. E. Valderrama, Performance analysis of machine learning models for human activity classification, *Engineered Science*, 2024, **31**, 1207, doi: 10.30919/es1207.
[35] J. AlShaqsi, M. Borghan, O. Drogham, G. H. Roshani, S. Al Whahaibi, Predicting pandemic fatality based on supervised machine learning methods, *Engineered Science*, 2024: **30**, 1169, doi: 10.30919/es1169.

[36] B. Mirza, W. Wang, J. Wang, H. Choi, N. C. Chung, P. Ping, Machine learning and integrative analysis of biomedical big data, *Genes*, 2019, **10**, 87, doi: 10.3390/genes10020087.
[37] T. Fan, Y. Li, Emissivity prediction of multilayer film radiators by machine learning using an ultrasmall dataset, *ES Energy & Environment*, 2022: **18**, 122–130, DOI: 10.30919/esee8c790.
[38] Q. Li, X.J. Yan, K. Zhao, L. Li, S.G. Peng, X. Luo, Y.S. Wen, Z.Y. Yan, Fast Inspection of Saffron on the Spot Based on Cloud-Connected Portable Near-Infrared Technology, *Spectroscopy and Spectral Analysis*, Science Press, 2020, **40**(10), 3029 - 3037, doi: 10.3964/J.ISSN.1000-0593(2020)10-3029-09.
[39] J. Charan, T. Biswas, How to Calculate Sample Size for Different Study Designs in Medical Research?, *Indian Journal of Psychological Medicine*, 2013, **35**, 121, doi: 10.4103/0253-7176.116232.
[40] S. Rattanamongkolgul, C. Wongjitrat, P. Puapankitcharoen, Prevalence of cirrhosis registered in Nakhon nayok, Thailand, *Journal of the Medical Association of Thailand*, 2010, **93**, 87-91.
[41] S. Chonprasertsuk, R.-K. Vilaichone, Epidemiology and treatment of hepatocellular carcinoma in Thailand, *Japanese Journal of Clinical Oncology*, 2017: **47**, 294–297, doi: 10.1093/jjco/hyw197.
[42] B. Buchard, Y. Boirie, L. Cassagnes, G. Lamblin, A. Coilly, A. Abergel, Assessment of malnutrition, sarcopenia and frailty in patients with cirrhosis: which tools should we use in clinical practice?, *Nutrients*, 2020, **12**, 186, doi: 10.3390/nu12010186.
[43] Y.-W. Lai, C.-H. Chung, Epidemiology of hepatocellular carcinoma in Taiwan, *Clinics and Practice*, 2024, **14**, 570-578, doi: 10.3390/clinpract14020044.
[44] M. Lampimukhi, T. Qassim, R. Venu, N. Pakhala, S. Mylavarapu, T. Perera, B. S. Sathar, A. Nair, A review of incidence and related risk factors in the development of hepatocellular carcinoma, *Cureus*, 2023: **15**(11), doi: 10.7759/cureus.49429.
[45] R. Nevola, G. Tortorella, V. Rosato, L. Rinaldi, S. Imbriani, P. Perillo, D. Mastrocinque, M. La Montagna, A. Russo, G. Di Lorenzo, M. Alfano, M. Rocco, C. Ricozzi, K. Gjeloshi, F. C. Sasso, R. Marfella, A. Marrone, L. A. Kondili, N. Esposito, E. Claar, D. Cozzolino, Gender differences in the pathogenesis and risk factors of hepatocellular carcinoma, *Biology*, 2023, **12**, 984, doi: 10.3390/biology12070984.
[46] T. Minamikawa, M. Ichimura-Shimizu, H. Takanari, Y. Morimoto, R. Shiomi, H. Tanioka, E. Hase, T. Yasui, K. Tsuneyama, Molecular imaging analysis of microvesicular and macrovesicular lipid droplets in non-alcoholic fatty liver disease by Raman microscopy, *Scientific Reports*, 2020, **10**, 18548, doi: 10.1038/s41598-020-75604-6.
[47] T. T. Nguyen, C. Gobinet, J. Feru, S. B.-Pasco, M. Manfait, O. Piot, Characterization of type I and IV collagens by Raman microspectroscopy: identification of spectral markers of the dermo-epidermal junction, *Journal of Spectroscopy*, 2012, **27**, 421-427, doi: 10.1155/2012/686183.
[48] Z. Movasaghi, S. Rehman, I. U. Rehman, Raman spectroscopy of biological tissues, *Applied Spectroscopy Reviews*, 2007, **42**, 493-541, doi: 10.1080/05704920701551530.
[49] É. Lemoine, F. Dallaire, R. Yadav, R. Agarwal, S. Kadoury, D. Trudel, M.-C. Guiot, K. Petrecca, F. Leblond, Feature engineering applied to intraoperative *in vivo* Raman spectroscopy sheds light on molecular processes in brain cancer: a retrospective study of 65 patients, *Analyst*, 2019, **144**, 6517-6532, doi: 10.1039/c9an01144g.
[50] C. Ma, L. Zhang, T. He, H. Cao, X. Ren, C. Ma, J. Yang, R. Huang, G. Pan, Single cell Raman spectroscopy to identify different stages of proliferating human hepatocytes for cell therapy, *Stem Cell Research & Therapy*, 2021, **12**, 555, doi: 10.1186/s13287-021-02619-9.
[51] F. E. R. Woods, S. Chandler, N. Sikora, R. Harford, A. Souriti, H. Gray, H. Wilkes, C. Lloyd-Bennett, D. A. Harris, P. R. Dunstan, An observational cohort study to evaluate the use of serum Raman spectroscopy in a rapid diagnosis center setting, *Clinical Spectroscopy*, 2022, **4**, 100020, doi: 10.1016/j.clispe.2022.100020.
[52] G. Pezzotti, Raman spectroscopy in cell biology and microbiology, *Journal of Raman Spectroscopy*, 2021, **52**, 2348-2443, doi: 10.1002/jrs.6204.
[53] M. G. Martinez, A. J. Bullock, S. MacNeil, I. U. Rehman, Characterisation of structural changes in collagen with Raman spectroscopy, *Applied Spectroscopy Reviews*, 2019, **54**, 509-542, doi: 10.1080/05704928.2018.1506799.
[54] W. S. Hong, S. I. Hong, S. Y. Park, Y. Son, Y. S. Lee, Y. H. Chung, S. K. Yang, D. J. Suh, Y. I. Min, Elevation of serum type IV collagen in liver cancer as well as liver cirrhosis, *Anticancer Research*, 1995, **15**, 2777-2780.
[55] C. Hirayama, H. Suzuki, A. Takada, K. Fujisawa, K. Tanikawa, S. Igarashi, Serum type IV collagen in various liver diseases in comparison with serum 7S collagen, laminin, and type III procollagen peptide, *Journal of Gastroenterology*, 1996, **31**, 242-248, doi: 10.1007/BF02389524.
[56] A. Niu, T. Qi, Diagnostic significance of serum type IV collagen (IVC) combined with aspartate aminotransferase (AST)/alanine aminotransferase (ALT) ratio in liver fibrosis, *Annals of Translational Medicine*, 2022, **10**, 1310, doi: 10.21037/atm-22-5010.
[57] S. E. Ghanem, M. Abdel-Samiee, H. El-Said, M. I. Youssef, H. A. ElZohry, E. Abdelsameea, I. Moaz, S. F. Abdelwahab, S. A. Elaskary, E. M. Zaher, M. L. Helal, Evaluation of amino acids profile as non-invasive biomarkers of hepatocellular carcinoma in Egyptians, *Tropical Medicine and Infectious Disease*, 2022, **7**, 437, doi: 10.3390/tropicalmed7120437.
[58] Z.-G. Gong, W. Zhao, J. Zhang, X. Wu, J. Hu, G.-C. Yin, Y.-J. Xu, Metabolomics and eicosanoid analysis identified serum biomarkers for distinguishing hepatocellular carcinoma from hepatitis B virus-related cirrhosis, *Oncotarget*, 2017, **8**, 63890-63900, doi: 10.18632/oncotarget.19173.
[59] P. H. Ooi, S. M. Gilmour, J. Yap, D. R. Mager, Effects of branched chain amino acid supplementation on patient care outcomes in adults and children with liver cirrhosis: A systematic review, *Clinical Nutrition ESPEN*, 2018, **28**, 41-51, doi: 10.1016/j.clnesp.2018.07.012.

[60] E. Moustafa, E. Hassan, M. Mahmoud, A. Mahmoud, M. A. A. Ghaliony, Deranged lipid profiles and hepatocellular carcinoma: clinical significance and association, *Middle East Journal of Cancer*, 2021, doi: 10.30476/MEJC.2021.86476.1346.
[61] D. Athavale, S. Chouhan, V. Pandey, S. S. Mayengbam, S. Singh, M. K. Bhat, Hepatocellular carcinoma-associated hypercholesterolemia: involvement of proprotein-convertase-subtilisin-kexin type-9 (PCSK9), *Cancer & Metabolism*, 2018, **6**, 16, doi: 10.1186/s40170-018-0187-2.
[62] Y. Kataria, R. J. Deaton, E. Enk, M. Jin, M. Petrauskaite, L. Dong, J. R. Goldenberg, S. J. Cotler, D. M. Jensen, R. B. van Breemen, P. H. Gann, Retinoid and carotenoid status in serum and liver among patients at high-risk for liver cancer, *BMC Gastroenterology*, 2016, **16**, 30, doi: 10.1186/s12876-016-0432-5.
[63] O. Pickett-Blakely, K. Young, R. M. Carr, Micronutrients in nonalcoholic fatty liver disease pathogenesis, *Cellular and Molecular Gastroenterology and Hepatology*, 2018, **6**, 451-462, doi: 10.1016/j.jcmgh.2018.07.004.
[64] P. Li, C. Chen, X. Deng, H. Mao, S. Jin, Drop coating deposition Raman spectroscopy of blood plasma for the detection of colorectal cancer, *Journal of Biomedical Optics*, 2015, **20**, 037004, doi: 10.1117/1.jbo.20.3.037004.
[65] S. Khan, R. Ullah, S. Shahzad, S. Javaid, A. Khan, Optical screening of nasopharyngeal cancer using Raman spectroscopy and support vector machine, *Optik*, 2018, **157**, 565-570, doi: 10.1016/j.ijleo.2017.11.097.
[66] A. Huang, H. Liu, Y. Pan, The antioxidant ability and extraction yield of beta carotene, *Highlights in Science, Engineering and Technology*, 2023, **58**, 256-264, doi: 10.54097/hset.v58i.10094.
[67] R. D. Clugston, Carotenoids and fatty liver disease: current knowledge and research gaps, *Biochimica et Biophysica Acta (BBA) - Molecular and Cell Biology of Lipids*, 2020, **1865**, 158597, doi: 10.1016/j.bbalip.2019.158597.
[68] L. I. Elvira-Torales, J. García-Alonso, M. J. Periago-Castón, Nutritional importance of carotenoids and their effect on liver health: a review, *Antioxidants*, 2019, **8**, 229, doi: 10.3390/antiox8070229.
[69] D.-M. Zhang, Y. Luo, D. Yishake, Z.-Y. Liu, T.-T. He, Y. Luo, Y.-J. Zhang, A.-P. Fang, H.-L. Zhu, Prediagnostic dietary intakes of vitamin A and β-carotene are associated with hepatocellular-carcinoma survival, *Food & Function*, 2020, **11**, 759-767, doi: 10.1039/c9fo02468a.
[70] I. Tougui, A. Jilbab, J. E. Mhamdi, Impact of the choice of cross-validation techniques on the results of machine learning-based diagnostic applications, *Healthcare Informatics Research*, 2021, **27**, 189-199, doi: 10.4258/hir.2021.27.3.189.
[71] M. Rosenblatt, L. Tejavibulya, R. Jiang, S. Noble, D. Scheinost, The effects of data leakage on neuroimaging predictive models, *bioRxiv*, 2023, doi: 10.1101/2023.06.09.544383.
[72] Dewinda J. Rumala, How You Split Matters: Data Leakage and Subject Characteristics Studies in Longitudinal Brain MRI Analysis, *arXiv.org*, 2023, **14242**, 235–245, doi: 10.48550/ARXIV.2309.00350.
[73] R. Mahalingam, D. Jayanthi K, High dimensionality reduction induced predictive modelling to enhance performance in decision support system. *Futuristic Trends in Computing Technologies and Data Sciences Volume 3 Book 6*, Iterative International Publishers, Selfypage Developers Pvt Ltd, 2024, **3**, 107-121, doi: 10.58532/v3bict6p6ch1.
[74] J. A. Ladenheim, D. G. Luba, F. Yao, P. B. Gregory, R. B. Jeffrey, G. Garcia, Limitations of liver surface US in the diagnosis of cirrhosis, *Radiology*, 1992, **185**, 21-23, doi: 10.1148/radiology.185.1.1523310.
[75] K. Y. Elbanna, A. Z. Kielar, Computed tomography versus magnetic resonance imaging for hepatic lesion characterization/diagnosis, *Clinical Liver Disease*, 2021, **17**, 159-164, doi: 10.1002/cld.1089.
[76] P. R. Galle, A. Forner, J. M. Llovet, V. Mazzaferro, F. Piscaglia, J.-L. Raoul, P. Schirmacher, V. Vilgrain, EASL Clinical Practice Guidelines: Management of hepatocellular carcinoma, *Journal of Hepatology*, 2018, **69**, 182-236, doi: 10.1016/j.jhep.2018.03.019.
[77] N. D. Parikh, M. Mehta, E. B. Tapper, FIB-4 and APRI for cirrhosis detection in a privately insured national cohort, *JHEP Reports*, 2024, **6**, 100925, doi: 10.1016/j.jhepr.2023.100925.
[78] T.-Y. Jang, C.-Y. Dai, Cutoff values of protein induced by vitamin K absence or antagonist II for diagnosing hepatocellular carcinoma, *Medicine*, 2022, **101**, e30936, doi: 10.1097/MD.0000000000030936.
[79] J. Zhang, G. Chen, P. Zhang, J. Zhang, X. Li, D.-N. Gan, X. Cao, M. Han, H. Du, Y.-A. Ye, The threshold of alpha-fetoprotein (AFP) for the diagnosis of hepatocellular carcinoma: A systematic review and meta-analysis, *PLoS One*, 2020, **15**, e0228857, doi: 10.1371/journal.pone.0228857.
[80] Y.-H. Yen, F.-Y. Kuo, C.-H. Chen, T.-H. Hu, S.-N. Lu, J.-H. Wang, C.-H. Hung, Ultrasound is highly specific in diagnosing compensated cirrhosis in chronic hepatitis C patients in real world clinical practice, *Medicine*, 2019, **98**, e16270, doi: 10.1097/MD.0000000000016270.
[81] H. Hu, Y. Zhao, C. He, L. Qian, P. Huang, Ultrasonography of Hepatocellular Carcinoma: From Diagnosis to Prognosis, *Xia & He Publishing Inc.*, 2024, **12**, 516–524, doi: 10.14218/JCTH.2024.00018.
[82] K. Tzartzeva, J. Obi, N. E. Rich, N. D. Parikh, J. A. Marrero, A. Yopp, A. K. Waljee, A. G. Singal, Surveillance imaging and alpha fetoprotein for early detection of hepatocellular carcinoma in patients with cirrhosis: a meta-analysis, *Gastroenterology*, 2018, **154**, 1706-1718.e1, doi: 10.1053/j.gastro.2018.01.064.
[83] A. G. Singal, H. S. Conjeevaram, M. L. Volk, S. Fu, R. J. Fontana, F. Askari, G. L. Su, A. S. Lok, J. A. Marrero, Effectiveness of hepatocellular carcinoma surveillance in patients with cirrhosis, *Cancer Epidemiology, Biomarkers & Prevention*, 2012, **21**, 793-799, doi: 10.1158/1055-9965.EPI-11-1005.
[84] K. G. King, J. Depetris, M. K. Patel, S. S. Raman, D. S. Lu, Contrast-enhanced ultrasound for hepatocellular carcinoma detection and diagnosis in the context of nonalcoholic fatty liver disease, *Hepatoma Research*, 2023, **9**, 8, doi: 10.20517/2394-5079.2022.49.

[85] Agency for Healthcare Research and Quality (AHRQ), Imaging Techniques for the Diagnosis and Staging of Hepatocellular Carcinoma, *Comparative Effectiveness Review Number 143*, *AHRQ*, n.d.
[86] A. Ronzoni, D. Artioli, R. Scardina, L. Battistig, E. Minola, S. Sironi, A. Vanzulli, Role of MDCT in the diagnosis of hepatocellular carcinoma in patients with cirrhosis undergoing orthotopic liver transplantation, *AJR. American Journal of Roentgenology*, 2007, **189**, 792-798, doi: 10.2214/AJR.07.2040.
[87] L. Lu, X. Pan, Accuracy of non-contrast MRI for the detection of hepatocellular carcinoma: a systematic review and meta-analysis, *Pakistan Journal of Medical Sciences*, 2022, **38**, 743-750, doi: 10.12669/pjms.38.3.5142.
[88] M. V. Chan, Y. R. Huo, N. Trieu, A. Mitchelle, J. George, E. He, A. U. Lee, J. Chang, J. Yang, Noncontrast MRI for hepatocellular carcinoma detection: a systematic review and meta-analysis - A potential surveillance tool? *Clinical Gastroenterology and Hepatology*, 2022, **20**, 44-56.e2, doi: 10.1016/j.cgh.2021.02.036.
[89] X.-X. Geng, R.-G. Huang, J.-M. Lin, N. Jiang, X.-X. Yang, Transient elastography in clinical detection of liver cirrhosis: A systematic review and meta-analysis, *Saudi Journal of Gastroenterology*, 2016, **22**, 294-303, doi: 10.4103/1319-3767.187603.
[90] P. Malik, S. Pillai, K. Agarwal, S. Abdelwahed, R. Bhandari, A. Singh, A. Chidharla, K. Patel, P. Singh, P. Manaktala, R. Rabbani, T. Koritala, S. Gupta, Diagnostic Accuracy of Elastography and Liver Disease: A Meta-Analysis, *Gastroenterology Research*, Elmer Press, Inc., 2022, **15**, 232, doi: 10.14740/GR1557.
[91] L. Di Tommaso, M. Spadaccini, M. Donadon, N. Personeni, A. Elamin, A. Aghemo, A. Lleo, Role of liver biopsy in hepatocellular carcinoma, *World Journal of Gastroenterology*, 2019, **25**, 6041-6052, doi: 10.3748/wjg.v25.i40.6041.
[92] E. S. Bialecki, A. M. Ezenekwe, E. M. Brunt, B. T. Collins, T. B. Ponder, B. K. Bieneman, A. M. Di Bisceglie, Comparison of liver biopsy and noninvasive methods for diagnosis of hepatocellular carcinoma, *Clinical Gastroenterology and Hepatology*, 2006, **4**, 361-368, doi: 10.1016/S1542-3565(05)00977-8.
[93] P. Gopal, A. C. Yopp, A. K. Waljee, J. Chiang, M. Nehra, P. Kandunoori, A. G. Singal, Factors that affect accuracy of α-fetoprotein test in detection of hepatocellular carcinoma in patients with cirrhosis, *Clinical Gastroenterology and Hepatology*, 2014, **12**, 870-877, doi: 10.1016/j.cgh.2013.09.053.
[94] R. Yu, X. Xiang, Z. Tan, Y. Zhou, H. Wang, G. Deng, Efficacy of PIVKA-II in prediction and early detection of hepatocellular carcinoma: a nested case-control study in Chinese patients, *Scientific Reports*, 2016, **6**, 35050, doi: 10.1038/srep35050.
[95] S.I. Seo, H.S. Kim, W.J. Kim, W.G. Shin, D.J. Kim, K.H. Kim, M.K. Jang, J.H. Lee, J.S. Kim, H.Y. Kim, D.J. Kim, M.S. Lee, C.K. Park, Diagnostic value of PIVKA-II and alpha-fetoprotein in hepatitis B virus-associated hepatocellular carcinoma, *World Journal of Gastroenterology: WJG*, WJG Press, 2015, **21**, 3928, doi: 10.3748/WJG.V21.I13.3928.
[96] E. S. Jang, S. H. Jeong, J. W. Kim, Y. S. Choi, P. Leissner, C. Brechot, Diagnostic performance of alpha-fetoprotein, protein induced by vitamin K absence, osteopontin, dickkopf-1 and its combinations for hepatocellular carcinoma, *PLoS One*, 2016, **11**, e0151069, doi: 10.1371/journal.pone.0151069.
[97] T. Suttichaimongkol, M. Mitpracha, K. Tangvoraphonkchai, P. Sadee, K. Sawanyawisuth, W. Sukeepaisarnjaroen, PIVKA-II or AFP has better diagnostic properties for hepatocellular carcinoma diagnosis in high-risk patients, *Journal of Circulating Biomarkers*, 2023, **12**, 12-16, doi: 10.33393/jcb.2023.2453.
[98] M. Bhusal, R. Pathak, B. Kafle Bhandari, A. Jha, R. Hamal, D. Koirala, M. Lamsal, P. K. Kafle, Liver cirrhosis among young adults admitted to the department of gastroenterology in a tertiary care centre: a descriptive cross-sectional study, *JNMA; Journal of the Nepal Medical Association*, 2023, **61**, 115-118, doi: 10.31729/jnma.8016.
[99] S. Wang, Z. Rao, R. Cao, A. H. Blaes, J. Coresh, C. E. Joshu, B. Lehallier, P. L. Lutsey, J. S. Pankow, S. Sedaghat, W. Tang, B. Thyagarajan, K. A. Walker, P. Ganz, E. A. Platz, W. Guan, A. Prizment, Development and characterization of proteomic aging clocks in the atherosclerosis risk in communities (ARIC) study, *medRxiv*, 2023, 2023.09.06.23295174, doi: 10.1101/2023.09.06.23295174.
[100] D. Appiah, P. J. Schreiner, J. S. Pankow, G. Brock, W. Tang, F. L. Norby, E. D. Michos, C. M. Ballantyne, A. R. Folsom, Long-term changes in plasma proteomic profiles in premenopausal and postmenopausal Black and White women: the Atherosclerosis Risk in Communities study, *Menopause*, 2022, **29**, 1150-1160, doi: 10.1097/GME.0000000000002031.
[101] G. S. Temba, N. Vadaq, V. Kullaya, T. Pecht, P. Lionetti, D. Cavalieri, J. L. Schultze, R. Kavishe, L. A. B. Joosten, A. J. van der Ven, B. T. Mmbaga, M. G. Netea, Q. de Mast, Differences in the inflammatory proteome of East African and Western European adults and associations with environmental and dietary factors, *eLife*, 2023, **12**, e82297, doi: 10.7554/elife.82297.
[102] G. S. Temba, N. Vadaq, V. Kullaya, T. Pecht, P. Lionetti, D. Cavalieri, J. L. Schultze, R. Kavishe, L. A. B. Joosten, A. J. van der Ven, B. T. Mmbaga, M. G. Netea, Q. de Mast, Differences in the inflammatory proteome of East African and Western European adults and associations with environmental and dietary factors, *eLife*, 2023, **12**, e82297, doi: 10.7554/eLife.82297.
[103] J. Duan, C. E. Vargas, N. Y. Yu, B. S. Laughlin, D. Santos Toesca, S. Keole, J. C. M. Rwigema, W. W. Wong, S. E. Schild, X. Feng, Q. Chen, Y. Rong, Incremental retraining, clinical implementation, and acceptance rate of deep learning auto-segmentation for male pelvis in a multiuser environment, *Medical Physics*, 2023, **50**, 4079-4091, doi: 10.1002/mp.16537.
[104] L. Faust, P. Wilson, S. Asai, S. Fu, H. Liu, X. Ruan, C. Storlie, Considerations for quality control monitoring of machine learning models in clinical practice, *JMIR Medical Informatics*, 2024, **12**, e50437, doi: 10.2196/50437.

and institutional affiliations.